IOP Publishing Journal of Physics: Condensed Matter
J. Phys.: Condens. Matter **32** (2020) 235101 (6pp) https://doi.org/10.1088/1361-648X/ab76ac

Measurement of viscoelastic properties of the cellular cytoplasm using optically trapped Brownian probes

Rahul Vaippully, Vaibavi Ramanujan, Saumendra Bajpai and Basudev Roy

Indian Institute of Technology, Madras, India

E-mail: basudev@iitm.ac.in

Received 4 November 2019, revised 29 January 2020
Accepted for publication 14 February 2020
Published 12 March 2020

Abstract

Measurement of the viscoelastic properties of a cell using microscopic tracer particles has been complicated given that the medium viscosity is dependent upon the size of the measurement probe leading to reliability issues. Further, a technique for direct calibration of optically trapped particles *in vivo* has been elusive due to the frequency dependence and spatial inhomogeneity of the cytoplasmic viscosity, and the requirement of accurate knowledge of the medium refractive index. Here, we employ a recent extension of Jeffery's model of viscoelasticity in the microscopic domain to fit the passive motional power spectra of micrometer-sized optically trapped particles embedded in a viscoelastic medium. We find excellent agreement between the 0 Hz viscosity in MCF7 cells and the typical values of viscosity in literature, between 2 to 16 mPa sec expected for the typical concentration of proteins inside the cytoplasmic solvent. This bypasses the dependence on probe size by relying upon small thermal displacements. Our measurements of the relaxation time also match values reported with magnetic tweezers, at about 0.1 s. Finally, we calibrate the optical tweezers and demonstrate the efficacy of the technique to the study of *in vivo* translational motion

Keywords: optical tweezers, in vivo rheology, viscoelastic cell cytoplasm

Supplementary material for this article is available online

(Some figures may appear in colour only in the online journal)

1. Introduction

Microrheology is the study of flow of matter at micron length scales and microliter sample volumes. It is particularly important when small quantities of materials are available, like in bio-physical studies. These can be performed in an environment where conventional rheological tools cannot reach inside the cells [1, 2]. Rheological characterization of cells is relevant for early diagnosis of diseases like malaria [3] and migration of cancerous cells [4]. The red blood cells (RBC) in malaria infected patients are known to have different elasticity than healthy ones. The extra-cellular matrix (ECM) of a cell in the human body interacts and changes the stiffness of the cytoskeleton in healthy cells via mechanical adaptation, the exact mechanism of which is not very well understood. A better match of the rheological features of the ECM and the cell is required for their adherence and cell mobility. Normally, when the ECM is too stiff and the cell cannot change its cytoskeletal features, there is no adherence. In the case of cancer cells, this mechanism is suppressed thereby allowing attachment inspite of stiffness mismatch and executes metastasis. Thus, one promising strategy to address cancer could be to understand and revive this cellular mechanism to match rheological features. In view of these facets, *in vivo* rheology is useful. Further, intracellular viscoelasticity has a role in diffusion of molecules and performance of chemical reactions, not to mention, such rheology also enables calibration of externally applied forces and torques on the system.

Recently, the cell cytoplasm was shown to be a poroelastic medium, [5] implying a medium with an elastic meshlike network into which a viscoelastic medium is suspended. There have been numerous attempts to ascertain the viscosity [6, 7], the refractive index [8, 9] and the viscoelasticity [10] of the cell cytoplasm. However, it is well known that the viscosity results are prone to the size of the probe used [11]. Any probe larger than 100 nm shall yield a viscosity larger than the native one, when probed actively. It is here, that a passive detection technique that moves the probe by small amounts can be expected to avoid the elastic mesh and provide information about the cytoplasmic fluid. Thus we study the passive thermal fluctuations of a probe using optical tweezers. Attempts to use optical tweezers *in vivo* [12–15] have been complicated due to the problems in quantifying the optical trap stiffness accurately [16], mainly due to the variable nature of the intracellular refractive index and the viscosity. We use a new theory to directly ascertain the unknown parameters and simultaneously calibrate it from the same fit 'at a glance'.

It is generally believed that the viscoelasticity of a medium automatically implies a segment-wise power-law behavior of the complex elastic modulus ($G^*(\omega) = A\omega^{\beta}$) in the frequency domain [17]. Recently, there has been an attempt to establish the macroscopic viscoelasticity of the medium from the microscopic Stokes Oldroyd-B model that showed a frequency-dependent viscosity quite akin to the Jeffery's model [18]. We use this new strategy to attack the problem of intra-cellular viscoelasticity and find that the motional power spectral density for spherical polystyrene particles of radius $a_0 = 0.5$ μm fits well to the suggested model. We extract the 0 Hz (DC) viscosity and find a good match with the established intra-cellular viscosity values. We also find the relaxation time of the intracellular medium, the optical trap stiffness and the calibration factor from the fitting parameters.

In conventional experiments for the calibration of the optical tweezers, the stage is modulated at a certain frequency and the thermal Brownian spectrum recorded. This typically bypasses the necessity for having an accurate pre-estimation of the diameter of the particle which can be automatically ascertained from such a calibration. The effect of the active calibration due to the motion of the stage is to add a sharp extra spike only at the frequency of the stage motion. However, inside cells, this active technique possibly induces cross coupling of the motion of the cytoplasmic fluid with the motion of the stage which adds extra noise to the power spectrum over a large band of frequencies. In the experiment performed in [14], the stage is modulated at 100 Hz while extra noise appears from 50 Hz to 250 Hz. Thus, a logical choice might be to not perform active stage modulation and use calibrated tracer particles, which is what we do.

2. Theory

The frequency- dependent viscosity in an incompressible low Reynolds number viscoelastic medium comprising of a solvent and a polymer solute dissolved in it has been found to be given by the following expression derived from the Stokes Oldroyd-B model for linear microscopic viscoelasticity [18]

$$\mu(\omega) = \mu_s + \frac{\mu_p}{-\mathrm{i}\omega\lambda + 1}. \tag{1}$$

Where μ_s is the zero frequency solvent viscosity, μ_p is the zero frequency polymer viscosity and λ is the polymer relaxation time. This expression is very similar to the Jeffery's model of frequency dependent viscosity with the coefficients labelled differently. Thus the viscosity of the solution at zero frequency would be, $\mu_0 = \mu_s + \mu_p$. Solving for the power spectral density of an optically trapped particle in a viscoelastic fluid, we get [18]

$$\langle x(\omega)x^*(\omega)\rangle = \frac{2k_{\mathrm{B}}T}{\gamma_0}\frac{(\frac{(1+\frac{\mu_p}{\mu_s})}{\lambda^2} + \omega^2)}{[(\frac{\kappa}{\gamma_0\lambda} - \omega^2)^2 + \omega^2(\frac{\kappa}{\gamma_0} + \frac{1}{\lambda}(1+\frac{\mu_p}{\mu_s}))^2]}. \tag{2}$$

The term κ signifies the trap stiffness and γ_0 is the drag coefficient for only the solvent. The exact expression for the γ_0 is given by,

$$\gamma_0 = 6\pi\mu_s a_0. \tag{3}$$

In order to correlate with experimentally obtained power spectral density curves of translational motion, we rewrite the equation (2), as

$$\langle x(\omega)x^*(\omega)\rangle = y_0 + \beta^2 A\frac{(\frac{(1+\frac{\mu_p}{\mu_s})}{\lambda^2} + \omega^2)}{[(\frac{\kappa}{\gamma_0\lambda} - \omega^2)^2 + \omega^2(\frac{\kappa}{\gamma_0} + \frac{1}{\lambda}(1+\frac{\mu_p}{\mu_s}))^2]} \tag{4}$$

where the A coefficient indicates the amplitude in terms of Volts^2 Hz^{-1} and the calibration factor is β in (m/Volt) quite akin to the conventional calibration factor for normal media [19]. The y_0 constant is added to the power spectra density to account for the system noise floor. The calibration factor for the translational signal is related to temperature as

$$\beta^2 A = \frac{2k_{\mathrm{B}}T}{\gamma_0}. \tag{5}$$

Thus, the calibration factor β is given as

$$\beta = \sqrt{\frac{2k_{\mathrm{B}}T}{A\gamma_0}}. \tag{6}$$

Fitting the power spectral density with this equation (4), we can extract the values of relative viscosity ($\frac{\mu_s+\mu_p}{\mu_s}$) of solution, polymer relaxation time constant (λ), the trap stiffness κ and the calibration factor β. The calibration factor only indicates how to scale between the V^2 Hz^{-1} to nm^2 Hz^{-1} and thus, to reduce the number of fitting parameters, we could normalise the curve to maximum to find all other parameters and then come back to this parameter later.

3. Experimental details

To perform the experiment, we place a polystyrene particle (1 ± 0.05 μm diameter, Thermo Fisher Scientific) inside a

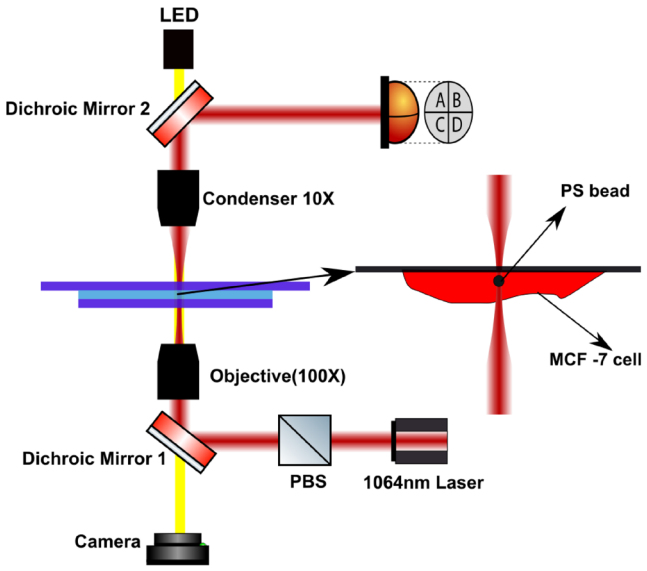

Figure 1. The schematic of the experimental set up. The MCF7 cell is attached to the top surface of a sample chamber with the probe particle located inside the cell. The optical tweezers light traps the particle and then the forward scattered light is used to perform translational measurements.

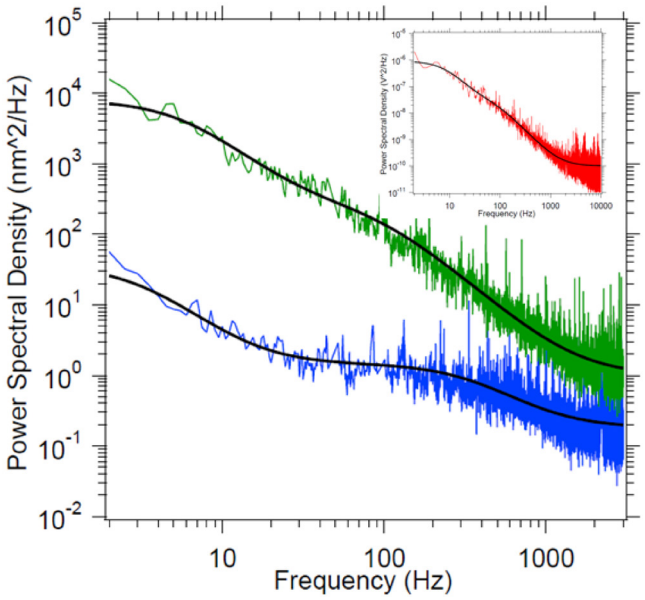

Figure 2. Power spectral density of the trapped particle fitted with the Oldroyd model, at different regimes of the same cell. The green curve indicates a typical PSD with DC viscosity about five times that of solvent, typically located close to the edges of the cell, while the blue curve indicates another location where it is 13 times that of solvent, typically located away from the periphery of the cell. We show that there are regions showing higher DC viscosity inside the same cell by more than a factor of two. The inset shows a typical fit using equation (4) to the case of a viscoelastic solution made from PAM in water.

cell attached to the glass slide (Blue Star, 75 mm length, 25 mm width and a thickness of 1.1 mm) of a sample chamber assembled, as shown in figure 1. The other side of the sample chamber is formed by a cover slip (Blue Star, number 1 size, english glass). The cell is close to the top surface of the sample chamber and illuminated in an inverted microscopy configuration using the Optical Tweezers kit (OTKB-M, Thorlabs USA) [20]. The illumination objective is a 1.3 NA, 100× oil immersion objective from Olympus at the bottom with the illumination aperture being overfilled. The collection objective at the top is E Plan 10×, 0.25 N.A. air-immersion objective from Nikon. The laser used for optical trapping is a diode laser from Lasever at 1064 nm wavelength which typically has a maximum power of 1.7 Watt with about 400 mW power in the sample plane. However, for the experiments performed in this manuscript, the laser was set to 200 mW power at the sample plane. An LED lamp illuminates the sample, coupled in using a dichroic mirror, as shown in figure 1. Another dichroic mirror couples the broadband visible light out of the path of the laser and illuminates a CMOS camera (Thorlabs, USA).

The translational motion is recorded by impinging the forward scattered light onto a quadrant photodiode (QPD) (Thorlabs, USA). This has four quadrants indicated by A, B, C, and D in figure 1. The top half minus the bottom half yields y displacement while the right half minus the left half yields the x displacement [21]. The bandwidth of this detector is 40 KHz. The position signals emerging from the QPD are acquired by the computer using data acquisition cards (National Instruments, NI PCI 6143) which has a bandwidth of 40 KHz.

We first tested that our technique works for a solution of polymers in water. For this, a concentrated solution of polyacrylamide (PAM, 1% by weight) was prepared in a water solvent with suspended 1 μm diameter polystyrene particles to make the viscoelastic solution [22]. One such particle was trapped, and the power spectral density of translational motion recorded with the optical tweezers system. The curve has been mentioned in the inset of figure 2 and fits well to the x-direction power spectral density dataset.

In order to create *in vivo* conditions, MCF-7 (Michigan Cancer Foundation-7) cells were grown on glass slides coated with gelatin. These glass slides were first treated with piranha solution and sterilized using UV (265 nm) light for 20 min and coated with 0.5% gelatin solution. MCF7 cells were added on to the center of the coverslip and Dulbecco's modified eagle medium (DMEM) supplemented with 10% fetal bovine serum and 1% glutamine-penicillin-streptomycin was added on top of the coverslip. 10 μl of gelatin-coated 0.5 μm radius polystyrene particles (1 μg ml^{-1}) suspended in sterile serum-free media were sonicated and added to the cells. The gelatin coating was done ourselves according to the standard procedures [23]. Cells were incubated with 5% carbondioxide and 37 °C for 24 h to initiate endocytosis [24] to insert the particles into the cell.

The temperature of the system was maintained using an air conditioner in the room at 26 °C, accurate to within 0.1 °C. Care was taken to ensure that the cool air from the air-conditioner was not blowing directly onto the system. In our experiments, the laser is placed on the particle and we wait for a minute for the conditions to stabilize. Then we take the measurement, which lasts for about 50 s, a period considered small enough to not alter the local environment of the particle. The room temperature is well controlled by the presence of the air

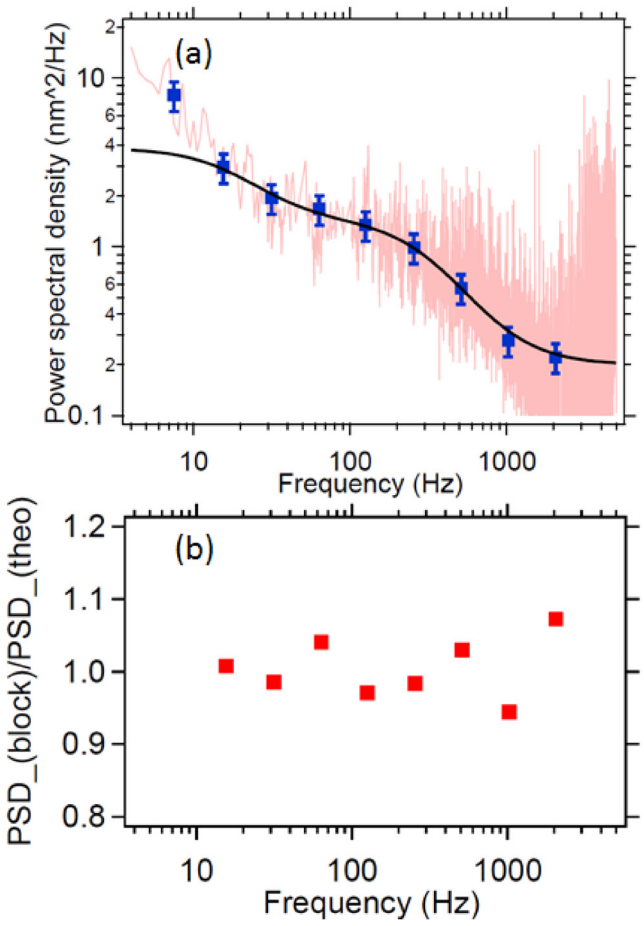

Figure 3. (a) A typical power spectral density (for the data shown in the blue curve of figure 2), block averaged logarithmically with a base of two, and fitted with the Oldroyd model. For convenience, the unaveraged data is also shown in the plot. (b) the ratio between the block averaged value and theoretical fit shows an agreement to within five percent. This fit is exclusively performed on the block averaged data.

conditioner. The only effects can be due to the presence of the laser on the particle, particularly in the local neighborhood of the particle. In our experiments, the laser is placed on the particle and we wait for a minute for the conditions to stabilize.

The particles incubated with the cells might either be outside the cell or inside. We ascertain this by first trapping the particle and then moving the stage back and forth manually in the X direction using micrometer screws by about 10 μm. If the particle is outside the cell and not residing on the membrane, it shall readily follow the trap without too much delay. If the particle is residing on the membrane and also non-specifically bound, it cannot follow the trap much. However, if the particle is indeed inside the cell, it follows the trap within the space available to it without hitting the side membrane or organelles like the nucleus. One such video has been shown in S1 (stacks.iop.org/JPhysCM/32/235101/mmedia). Once we ascertain the focus of the objective for which the particles can be trapped inside the cell, we mark it to find other particles at the same depth.

4. Results and discussions

A typical motional power spectral density for a particle inside a cell has been shown in figure 2. Every power spectra is calculated by taking a 5 s time series and averaging over 10 such spectra. The equation (4) fits well to the experimental data. The fitting parameters automatically yield the A parameter in volts^2 Hz^{-1} and subsequently the calibration factor β, as shown in equation (6). We also extract the ratios $\frac{\kappa}{\gamma_0}$ and $1+\frac{\mu_p}{\mu_s}$. We show two more datasets indicating PSD's at two different locations of the same cell in figure 2. The green curve shows a typical DC viscosity of five times that of solvent while the blue curve shows a value of 13 times that of solvent. There can be variations by factors of 2 to 3 inside the same cell. These spectra are also calibrated to indicate thermal motion at each frequency. We can see that the DC thermal motion is of the order of 100 nm which reduces to 3 nm at 1000 Hz. Thus, we typically achieve a frequency range of about 3000 Hz with our present configuration.

In order to estimate the quality of the fit, we have block averaged the data shown in figure 2 (blue) in logarithmic bins with a base of 2, meaning bins of sizes 1,2,4,8 and so on upto about 3 kHz, using the method reported by Berg–Sorensen *et al* [25]. Then we have fitted it with our Oldroyd model, shown in figure 3. We find that the ratio of the block averaged value to that obtained using the theoretical fit is within five percent, meaning between 0.95 and 1.05. Thus the fit is good to within an accuracy of five percent. The fit can be improved by logarithmic block averaging over larger blocks to get better estimates for the averaged bin values.

We also hypothesize that active motion due to the molecular motors etc inside the cell appears below 10 Hz, as indicated in figures 4 and 5 by Guo *et al* [26]. The PSD has a power law exponent of -2 at less than 10 Hz due to active motion [27], which is also what we observe in our case. Thus, we can use the remainder of the range to fit to thermal power spectra. Here, we can mention that there have been attempts to fit viscoelastic models to PSD due to thermal motion inside the cell [14] but the spectra have partially been ruined by the motion of the translation stage. When the stage has been actively moved at 100 Hz, technical noise appeared all the way from under 100 Hz–300 Hz. Thus active stage modulation would only complicate matters.

If we assume that the solvent medium for the cell is water, which has been proved to be a good approximation [28], the μ_s is automatically that of water while the γ_0 is given by equation (3). Using this approximation, we extract values for the DC viscosity $\mu_0+\mu_p$, indicated in figure 4(a) and λ, indicated in figure 4(b) for 58 different observations.

The DC (0 Hz) viscosity for the cell cytoplasm seems to vary from 2 mPa sec to 16 mPa sec, which is what one expects for typical intracellular concentrations of protein filaments like actin, microtubules and intermediate filaments dissolved in water [29]. In our experiments, with 200 mW laser power at the focus, we find that the particles are easier to trap, closer to the sides of the cell. Typically these are the regions where

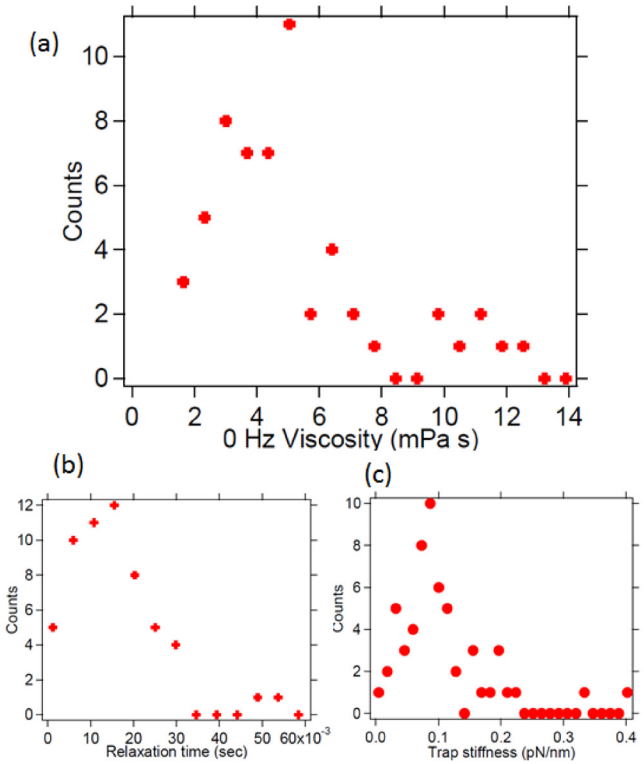

Figure 4. (a) The value of DC(0 Hz) viscosity for the cell cytoplasm for 58 number of observations. The average is 5.5 ± 3 mPa · s. (b) Measurement of polymer time constant λ for the passive motion of the probe particle in every 58 observations. The average is 0.02 s (c) This shows typical trap stiffness of 1 μm diameter polystyrene particles *in vivo*.

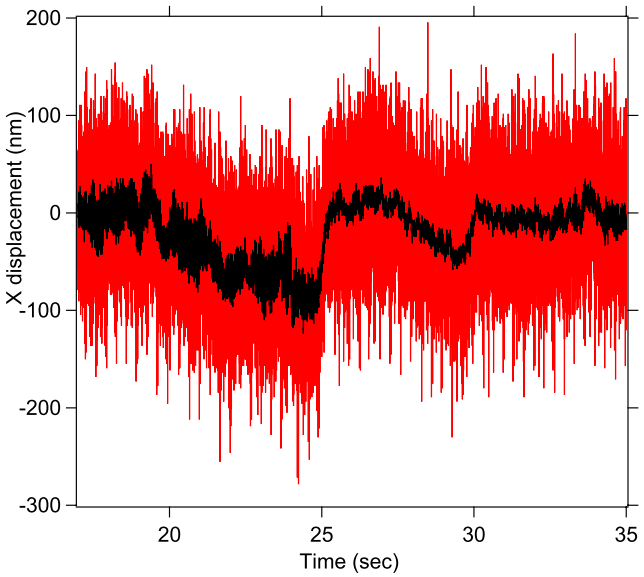

Figure 5. This figure indicates a calibrated x-position time series of a 1 μm diameter particle moving on a microtubule inside the cell. The red line indicates unfiltered data while the black curve indicated median filtered data. The force exerted by the molecular motors on the particle can be ascertained by multiplying the trap stiffness of 0.12 pN nm^{-1} (in this case) with the value of the displacement here.

we expect the cell to be less viscous. As we move away from the sides or edges of the cell, we generally find the viscosity higher. We also find that there are pockets even in the middle of the cell (away from edges or sides) where the viscosity is lower and some places which have more. Indeed we see a bimodal distribution in the 0 Hz viscosity values reported in figure 4(a). There is a band in the range of 2–6 times that of water which is possibly close to the sides and another band towards the middle and away from the sides where the viscosity is 10–12 times that of water. As soon as larger probes are used, however, the value appears orders of magnitude larger [30]. We speculate that since the cell is actually poroelastic in nature, the probes larger than 50 nm in size gets entangled in the cytoplasmic network and provides larger drag than experienced by smaller probes. This biases the viscosity measured towards higher values. In our experiments, we rely on small thermal fluctuations about the mean which are not large enough to experience the cytoplasmic poroelasticity. Further, the average relaxation time is 0.021 ± 0.005 s. A typical estimate using the Maxwell's model observed a value of 0.2 s [30]. The difference between the values of the relaxation times is possibly caused due to the different models used.

We also extract the typical trap stiffness at the same value of laser power of 200 mW at the sample plane, shown in figure 4(c). The trap stiffness seems to have an average value of 0.1 pN nm^{-1}. The expression for the trapping efficiency for a 1 μm diameter particle at 200 mW laser power and a medium refractive index of 1.5 is $\frac{kr_1c}{n_1P} = 0.05$ [31], where k is the trap stiffness, c the speed of light, n_1 the refractive index, r_1 is the radius of particle and P the laser power.

In these measurements, we span a frequency range between 2 Hz and 3000 Hz, partly including the athermal fluctuations inside the cell ranging from 0.1 Hz to 10 Hz [32]. Indeed we find deviations from the thermal curve below 10 Hz, as shown in figure 2. Moreover, as indicated by Tassieri [33], the tweezers can indeed probe the viscoelasticity of the cell if the measurement time is lower than active motion time, given by the Deborah number (De) being greater than 1. Since we have a frequency range extending to 3 KHz, the measurement time is indeed smaller than 10 Hz activity time, thus enabling this kind of approach. Once the optical tweezers is calibrated properly, newer experiments could even be designed to look specifically at the athermal fluctuations.

We also calibrate a typical time series for the x displacement of a 1 μm diameter microsphere inside the cell, while being carried by molecular motors on microtubules. It has been shown in figure 5. The red curve shows the unfiltered data while the black curve shows a median filtered data. The optical trap stiffness in this case was 0.12 pN nm^{-1}. Thus the force applied by the molecular motors on the particle is then about 10 pN, possibly indicating multiple motors at work.

5. Conclusions

In conclusion, we have trapped 1 μm diameter polystyrene particle inside MCF-7 cells and obtained the power spectral density for passive motion of the particle along the x-axis inside the cell. To fit the PSD, we model the cytoplasm as a polymer

network immersed in water that acts as a viscoelastic medium. This power spectrum is fitted with Jefferey's model. We see that the relative viscosity, polymer relaxation time and the trap stiffness varies inside the cell from place to place possibly due to the variation of cytoplasmic density, but maintains a good agreement with previous literature. This study of the viscoelasticity of the cell is made possible by the enhanced frequency response due to the power spectral density extending to 3 KHz, thereby ensuring a Deborah number greater than one, when compared with activity frequency of 5 Hz or slower.

Acknowledgments

We thank the Indian Institute of Technology Madras, India for their seed Grant.

Author contributions

BR and SB designed the experiment. RV, SRV and BR performed the experiment and did data analysis. BR and SB wrote the manuscript.

ORCID iDs

Basudev Roy https://orcid.org/0000-0003-0737-2889

References

[1] Kollmansberger P and Fabry B 2011 *Annu. Rev. Mater. Res.* **41** 75–97
[2] Harrison A W, Kenwright D A, Waigh T A, Woodman P G and Allan V J 2013 *Phys. Biol.* **10** 036002
[3] Crick A, Tiffert T, Shah S, Kotar J, Lew V L and Cicuta P 2013 *Biophys. J.* **104** 997–1005
[4] Staunton J R, So W Y, Paul C D and Tanner K 2019 *Proc. Natl Acad. Sci.* **116** 14448–55
[5] Hu J, Jafari S, Han Y, Grodzinsky A J, Cai S and Guo M 2017 *Proc. Natl Acad. Sci.* **114** 9529–34
[6] Puchkov E O 2013 *Biochem. Supp. Ser. A: Membr. Cell. Biol.* **7** 270–9
[7] Kuimova M K, Botchway S W, Parker A W, Balaz M, Collins H A, Anderson H L, Suhling K and Ogilby P R 2009 *Nat. Chem.* **1** 69–73
[8] Vinoth B, Lai X J, Lin Y C, Tu H Y and Cheng C J 2018 *Sci. Rep.* **8** 5943
[9] Kim K and Park Y 2017 *Nat. Commun.* **8** 15340
[10] Berret J F 2016 *Nat. Commun.* **7** 10134
[11] Kalwarczyk T *et al* 2011 *Nano Lett.* **11** 2157–63
[12] Jeon J H, Tejedor V, Burov S, Barkai E, Selhuber-Unkel C, Berg-Sãÿrensen K, Oddershede L and Metzler R 2011 *Phys. Rev. Lett.* **106** 048103
[13] Barak P, Rai A, Rai P and Mallik R 2013 *Nat. Math.* **10** 68–70
[14] Hendricks A G, Holzbaur E L F and Goldman Y E 2012 *Proc. Natl Acad. Sci.* **109** 18447–52
[15] Mas J, Richardson A C, Reihani S N S, Oddershede L B and Berg-Sorensen K 2013 *Phys. Biol.* **10** 046006
[16] Jun Y, Tripathy S K, Narayanareddy B R J, Mattson-Hoss M K and Gross S P 2014 *Biophys. J.* **107** 1474–84
[17] Guigas G, Kalla C and Weiss M 2007 *Biophys. J.* **93** 316–23
[18] Paul S, Roy B and Banerjee A 2018 *J. Phys.: Condens. Matter* **30** 345101
[19] Schaffer E, Norrelykke S F and Howard J 2007 *Langmuir* **23** 3654–65
[20] Vaippully R, Bhatt D, Ranjan A D and Roy B 2019 *Phys. Scr.* **94** 105008
[21] Roy B, Bera S K and Banerjee A 2014 *Opt. Lett.* **39** 3316–9
[22] Paul S, Kundu A and Banerjee A 2019 *J. Phys. Commun.* **3** 035002
[23] Ratanavaraporn J, Chuma N, Kanokpanont S and Damrongsakkul S 2019 *J. Appl. Polym. Sci.* **136** 46893
[24] Hu J *et al* 2019 *Proc. Natl Acad. Sci. USA* **116** 17175–80
[25] Berg-Sorensen K and Flyvbjerg H 2004 *Rev. Sci. Instrum.* **75** 594–612
[26] Guo M, Ehrlicher A J, Jensen M H, Renz M, Moore J R, Goldman R D, Lippincott-Schwarz J, Macintosh F C and Weitz D A 2014 *Cell* **158** 822–32
[27] Gupta S K and Guo M 2017 *J. Mech. Phys. Solids* **107** 284–93
[28] Luby-Phelps K, Mujumdar S, Mujumdar R B, Ernst L A, Galbraith W and Waggone A S 1993 *Biophys. J.* **65** 236–42
[29] Wagner O, Zinke J, Dancker P, Grill W and Bereiter-Hahn J 1999 *Biophys. J.* **76** 2784–96
[30] Bausch A R, Moller W and Sackmann E 1999 *Biophys. J.* **76** 573–9
[31] Malagnino N, Pesce G, Sasso A and Arimondo E 2002 *Opt. Commun.* **214** 15–24
[32] Toyota T, Head D A, Schmidt C F and Mizuno D 2011 *Soft Matter* **7** 3234–9
[33] Tassieri M 2015 *Soft Matter* **11** 5792–8